



HAL
open science

Solid-state NMR sequential assignments of the N-terminal domain of HpDnaB helicase

Thomas Wiegand, Carole Gardiennet, Francesco Ravotti, Alexandre Bazin,
Britta Kunert, Denis Lacabanne, Riccardo Cadalbert, Peter Güntert, Laurent
Terradot, Anja Böckmann, et al.

► To cite this version:

Thomas Wiegand, Carole Gardiennet, Francesco Ravotti, Alexandre Bazin, Britta Kunert, et al..
Solid-state NMR sequential assignments of the N-terminal domain of HpDnaB helicase. *Biomolecular
NMR Assignments*, 2016, 10 (1), pp.13 - 23. 10.1007/s12104-015-9629-8 . hal-01850802

HAL Id: hal-01850802

<https://hal.univ-lorraine.fr/hal-01850802>

Submitted on 27 Jul 2018

HAL is a multi-disciplinary open access archive for the deposit and dissemination of scientific research documents, whether they are published or not. The documents may come from teaching and research institutions in France or abroad, or from public or private research centers.

L'archive ouverte pluridisciplinaire **HAL**, est destinée au dépôt et à la diffusion de documents scientifiques de niveau recherche, publiés ou non, émanant des établissements d'enseignement et de recherche français ou étrangers, des laboratoires publics ou privés.

Dear Author,

Here are the proofs of your article.

- You can submit your corrections **online**, via **e-mail** or by **fax**.
- For **online** submission please insert your corrections in the online correction form. Always indicate the line number to which the correction refers.
- You can also insert your corrections in the proof PDF and **email** the annotated PDF.
- For fax submission, please ensure that your corrections are clearly legible. Use a fine black pen and write the correction in the margin, not too close to the edge of the page.
- Remember to note the **journal title**, **article number**, and **your name** when sending your response via e-mail or fax.
- **Check** the metadata sheet to make sure that the header information, especially author names and the corresponding affiliations are correctly shown.
- **Check** the questions that may have arisen during copy editing and insert your answers/ corrections.
- **Check** that the text is complete and that all figures, tables and their legends are included. Also check the accuracy of special characters, equations, and electronic supplementary material if applicable. If necessary refer to the *Edited manuscript*.
- The publication of inaccurate data such as dosages and units can have serious consequences. Please take particular care that all such details are correct.
- Please **do not** make changes that involve only matters of style. We have generally introduced forms that follow the journal's style. Substantial changes in content, e.g., new results, corrected values, title and authorship are not allowed without the approval of the responsible editor. In such a case, please contact the Editorial Office and return his/her consent together with the proof.
- If we do not receive your corrections **within 48 hours**, we will send you a reminder.
- Your article will be published **Online First** approximately one week after receipt of your corrected proofs. This is the **official first publication** citable with the DOI. **Further changes are, therefore, not possible.**
- The **printed version** will follow in a forthcoming issue.

Please note

After online publication, subscribers (personal/institutional) to this journal will have access to the complete article via the DOI using the URL: [http://dx.doi.org/\[DOI\]](http://dx.doi.org/[DOI]).

If you would like to know when your article has been published online, take advantage of our free alert service. For registration and further information go to: <http://www.link.springer.com>.

Due to the electronic nature of the procedure, the manuscript and the original figures will only be returned to you on special request. When you return your corrections, please inform us if you would like to have these documents returned.

Metadata of the article that will be visualized in OnlineFirst

ArticleTitle	Solid-state NMR sequential assignments of the N-terminal domain of <i>HpDnaB</i> helicase	
Article Sub-Title		
Article CopyRight	Springer Science+Business Media Dordrecht (This will be the copyright line in the final PDF)	
Journal Name	Biomolecular NMR Assignments	
Corresponding Author	Family Name	Terradot
	Particle	
	Given Name	L.
	Suffix	
	Division	Institut de Biologie et Chemie des Protéines, Bases Moléculaires et Structurales des Systèmes Infectieux, Labex Ecofect, UMR 5086 CNRS
	Organization	Université de Lyon
	Address	7 passage du Vercor, Lyon, 69007, France
	Email	laurent.terrardot@ibcp.fr
Corresponding Author	Family Name	Böckmann
	Particle	
	Given Name	A.
	Suffix	
	Division	Institut de Biologie et Chemie des Protéines, Bases Moléculaires et Structurales des Systèmes Infectieux, Labex Ecofect, UMR 5086 CNRS
	Organization	Université de Lyon
	Address	7 passage du Vercor, Lyon, 69007, France
	Email	a.bockmann@ibcp.fr
Corresponding Author	Family Name	Meier
	Particle	
	Given Name	B. H.
	Suffix	
	Division	Laboratorium für Physikalische Chemie
	Organization	ETH Zürich
	Address	Vladimir-Prelog-Weg 2, Zurich, 8093, Switzerland
	Email	beme@ethz.ch
Author	Family Name	Wiegand
	Particle	
	Given Name	T.
	Suffix	
	Division	Laboratorium für Physikalische Chemie
	Organization	ETH Zürich
	Address	Vladimir-Prelog-Weg 2, Zurich, 8093, Switzerland
	Email	
Author	Family Name	Gardiennet
	Particle	

Given Name **C.**
Suffix
Division Institut de Biologie et Chimie des Protéines, Bases Moléculaires et
Structurales des Systèmes Infectieux, Labex Ecofect, UMR 5086 CNRS
Organization Université de Lyon
Address 7 passage du Vercor, Lyon, 69007, France
Email

Author Family Name **Ravotti**
Particle
Given Name **F.**
Suffix
Division Laboratorium für Physikalische Chemie
Organization ETH Zürich
Address Vladimir-Prelog-Weg 2, Zurich, 8093, Switzerland
Email

Author Family Name **Bazin**
Particle
Given Name **A.**
Suffix
Division Institut de Biologie et Chimie des Protéines, Bases Moléculaires et
Structurales des Systèmes Infectieux, Labex Ecofect, UMR 5086 CNRS
Organization Université de Lyon
Address 7 passage du Vercor, Lyon, 69007, France
Email

Author Family Name **Kunert**
Particle
Given Name **B.**
Suffix
Division Institut de Biologie et Chimie des Protéines, Bases Moléculaires et
Structurales des Systèmes Infectieux, Labex Ecofect, UMR 5086 CNRS
Organization Université de Lyon
Address 7 passage du Vercor, Lyon, 69007, France
Email

Author Family Name **Lacabanne**
Particle
Given Name **D.**
Suffix
Division Laboratorium für Physikalische Chemie
Organization ETH Zürich
Address Vladimir-Prelog-Weg 2, Zurich, 8093, Switzerland
Division Institut de Biologie et Chimie des Protéines, Bases Moléculaires et
Structurales des Systèmes Infectieux, Labex Ecofect, UMR 5086 CNRS
Organization Université de Lyon
Address 7 passage du Vercor, Lyon, 69007, France
Division Institute of Biophysical Chemistry, Center for Biomolecular Magnetic
Resonance
Organization Goethe University Frankfurt am Main

	Address	Max-von-Laue-Str. 9, Frankfurt am Main, 60438, Germany
	Email	
Author	Family Name	Cadalbert
	Particle	
	Given Name	R.
	Suffix	
	Division	Laboratorium für Physikalische Chemie
	Organization	ETH Zürich
	Address	Vladimir-Prelog-Weg 2, Zurich, 8093, Switzerland
	Email	
Author	Family Name	Güntert
	Particle	
	Given Name	P.
	Suffix	
	Division	Laboratorium für Physikalische Chemie
	Organization	ETH Zürich
	Address	Vladimir-Prelog-Weg 2, Zurich, 8093, Switzerland
	Division	Institute of Biophysical Chemistry, Center for Biomolecular Magnetic Resonance
	Organization	Goethe University Frankfurt am Main
	Address	Max-von-Laue-Str. 9, Frankfurt am Main, 60438, Germany
	Email	
Schedule	Received	29 March 2015
	Revised	
	Accepted	11 August 2015
Abstract	<p>We present solid-state NMR assignments of the N-terminal domain of the DnaB helicase from <i>Helicobacter pylori</i> (153 residues) in its microcrystalline form. We use a sequential resonance assignment strategy based on three-dimensional NMR experiments. The resonance assignments obtained are compared with automated resonance assignments computed with the ssFLYA algorithm. An analysis of the ^{13}C secondary chemical shifts determines the position of the secondary structure elements in this α-helical protein.</p>	
Keywords (separated by '-')	HpDnaB - Assignments - Solid-state NMR - Secondary chemical shifts - ssFLYA	
Footnote Information	T. Wiegand and C. Gardiennet have equally contributed to this work.	

2 **Solid-state NMR sequential assignments of the N-terminal domain**
3 **of *HpDnaB* helicase**

4 T. Wiegand¹ · C. Gardiennet² · F. Ravotti¹ · A. Bazin² ·
5 B. Kunert² · D. Lacabanne^{1,2,3} · R. Cadalbert¹ · P. Güntert^{1,3} ·
6 L. Terradot² · A. Böckmann² · B. H. Meier¹

7 Received: 29 March 2015 / Accepted: 11 August 2015
8 © Springer Science+Business Media Dordrecht 2015

9 **Abstract** We present solid-state NMR assignments of the
10 N-terminal domain of the DnaB helicase from *Helicobac-*
11 **ter pylori** (153 residues) in its microcrystalline form. We
12 use a sequential resonance assignment strategy based on
13 three-dimensional NMR experiments. The resonance
14 assignments obtained are compared with automated reso-
15 nance assignments computed with the ssFLYA algorithm.
16 An analysis of the ¹³C secondary chemical shifts deter-
17 mines the position of the secondary structure elements in
18 this α -helical protein.

20 **Keywords** *HpDnaB* · Assignments · Solid-state NMR ·
21 Secondary chemical shifts · ssFLYA

Biological context

DnaB helicases are bacterial ATP-driven enzymes which
unwind double-stranded DNA in the presence of ATP
during the fork movement in 5'-3' direction in DNA
replication (LeBowitz and McMacken 1986). Structurally,
DnaB is a two-domain helicase with an amino-terminal
domain and a carboxy-terminal domain separated by a
linker region. The full-length protein forms ring-shaped
hexameric assemblies which encircle single-stranded DNA
(LeBowitz and McMacken 1986). The C-terminal domain
supports the ATPase activity and is involved in the ring
formation, while the N-terminal domain is forming an
 α -helical globule which has the function to activate the
helicase. A fundamental step in DNA replication is the
strand synthesis which is initiated by an interaction
between the N-terminal domain of the helicase DnaB and
the primase DnaG (Corn and Berger 2006).

This work focuses on the investigation of the N-termi-
nus of DnaB extracted from *Helicobacter pylori*
(*H. pylori*), a gram-negative microaerophilic spiral shaped
bacterium which is, with a worldwide prevalence of
approximately 50 %, responsible for the most common
chronic bacterial infections, such as gastric ulcer diseases
and gastric adenocarcinoma (Parsonnet et al. 1991; Peter-
son 1991). The replication system in *H. pylori* exhibits
significant differences compared to other microorganisms
which were investigated in detail, e.g. *Escherichia coli*.
The most relevant differences are the absence of the *recF*
gene, the presence of the *dnaA* gene ~600 kb away from
the *dnaN-gyrB* genes and most importantly the absence of
the *dnaC* gene (Soni et al. 2003). In *E. coli*, DnaC is
essential for loading DnaB helicase at *oriC*, which is the
origin of the chromosomal DNA replication, whereas in the
case of *H. pylori HpDnaB* itself is able to take over the

A1 T. Wiegand and C. Gardiennet have equally contributed to this work.

A2 L. Terradot
A3 laurent.terradot@ibcp.fr

A4 A. Böckmann
A5 a.boeckmann@ibcp.fr

A6 B. H. Meier
A7 beme@ethz.ch

A8 ¹ Laboratorium für Physikalische Chemie, ETH Zürich,
A9 Vladimir-Prelog-Weg 2, 8093 Zurich, Switzerland

A10 ² Institut de Biologie et Chimie des Protéines, Bases
A11 Moléculaires et Structurales des Systèmes Infectieux, Labex
A12 Ecofect, UMR 5086 CNRS, Université de Lyon, 7 passage du
A13 Vercoq, 69007 Lyon, France

A14 ³ Institute of Biophysical Chemistry, Center for Biomolecular
A15 Magnetic Resonance, Goethe University Frankfurt am Main,
A16 Max-von-Laue-Str. 9, 60438 Frankfurt am Main, Germany

56 DnaC function (Soni et al. 2005). The crystal structure of
 57 the C-terminal domain (Stelter et al. 2012), as well as of
 58 the 121 N-terminal residues of *HpDnaB* were determined
 59 (Kashav et al. 2009). The latter one was found to consist of
 60 a dimer and two further degradation peptide fragments in
 61 the asymmetric unit (Kashav et al. 2009). This manuscript
 62 presents the solid-state NMR spectroscopic investigation of
 63 the N-terminus of *HpDnaB* as a step towards an integrated
 64 structural biology approach aiming at a detailed structural
 65 description of the full-length protein. In this context, solid-
 66 state NMR studies on a sedimented sample of the full-
 67 length protein have been described (Gardiennet et al.
 68 2012). Previous biochemical investigations suggest that the
 69 N-terminal domain and the linker region play an important
 70 role in multimerisation, quaternary state transition and
 71 activity of *HpDnaB* (Kashav et al. 2009; Nitharwal et al.
 72 2007).

73 Methods and experiments

74 Protein expression and purification, sample 75 preparation

76 The DNA fragment corresponding to the N-terminal
 77 domain of the *H. pylori* helicase DnaB (strain 26695) was
 78 amplified by PCR (forward 5'-caccatggatcatttaaag-
 79 catttcgag-3' and reverse 5'-gcaccatagaaggcttaggaattag-3')
 80 from genomic DNA and inserted into the plasmid pET151/
 81 DTopo (Invitrogen™). The resulting vector was intro-
 82 duced into *E. coli* BL21(DE3) cells (One Shot® BL21
 83 Star™ (DE3) Chemically Competent *E. coli*, Invitro-
 84 gen™) and protein overexpression was performed in
 85 minimal M9 medium (Studier 2005) containing D-[U-¹³-
 86 C]glucose 2 g L⁻¹ (Cambridge Isotope Laboratories, Inc.
 87 CLM-1396-PK) and ¹⁵NH₄Cl 2 g L⁻¹ (Sigma-Aldrich®
 88 299251) as the only nitrogen and carbon sources. After cell
 89 lysis by a microfluidization process, ¹³C-¹⁵N-DnaB-Nter
 90 was purified by Ni²⁺-agarose affinity chromatography
 91 (Qiagen™). The pseudo-affinity tag was subsequently
 92 cleaved with the TEV (Tobacco Etch Virus) protease by
 93 dialysis. Six additional residues of the tag remain in the
 94 sequence (see Fig. 1).

95 For crystallization, ¹³C-¹⁵N-DnaB-Nter was concen-
 96 trated to 23.5 mg/ml using a centrifugal concentrator with
 97 a 10 kDa cut-off (Vivaspin® 20 VS2001 Sartorius), and the
 98 buffer was exchanged during the concentration step with
 99 the final buffer (50 mM Tris-HCl pH 6.5, 100 mM NaCl).
 100 Crystallization of the protein was performed by mixing an
 101 equal volume of protein and crystallization buffer
 102 (100 mM HEPES pH 7.0, 0.1 % (m/v) sodium azide, 10 %
 103 (v/v) polyethylene glycol 10000) in a nine-well glass plate
 104 with 2.3 M NaCl solution in the reservoir. Microcrystals

```

  0
  GIDPFT
  10      20      30      40      50      60
  MDHLKHLQL QNIERIVLGG IVLANHKIEE VHSVLEPSDF YYPNGLFFE IALKLHEEDC
  70      80      90     100     110     120
  PIDENFIRQK MPKDKQIKEE DLVAIFAAASP IDNIEAYVEE IKNASIKRKL FGLANTIREQ
  130     140     150
  ALESAQKSSD ILGAVEREYV ALLNGSTIEG FRN
  
```

Fig. 1 Amino-acid sequence of the N-terminus of *HpDnaB* as extracted from the uniprot database (The UniProt Consortium-Activities at the Universal Protein Resource (UniProt) 2014). At the N-terminal domain a part of the tag (amino acid sequence GIDPFT) is still present after the cleavage of the tag with TEV protease (shown in grey). Residues highlighted in red are located in α -helices as determined from NMR secondary chemical shifts (see Fig. 9)

were obtained after 1 week at 20 °C and were harvested 105
 and centrifuged into the NMR rotor (25,000×g during 1 h 106
 at 4 °C) using a homemade device (Böckmann et al. 2009). 107

Solid-state NMR spectroscopy 108

Solid-state NMR spectra were acquired at 18.8 and 20.0 T 109
 static magnetic field strengths using 3.2 mm Bruker Bios- 110
 pin “E-free” probes (Gor’kov et al. 2007). The MAS 111
 spinning frequency was set to 17.5 and 17.0 kHz for the 112
 two fields, respectively. The 2D and 3D spectra were 113
 processed with the software TOPSPIN (version 3.2, Bruker 114
 Biospin) with a shifted (2.0–2.8) squared cosine apodiza- 115
 tion function and automated baseline correction in the 116
 direct dimension. The sample temperature was set to 117
 278 K, for more details of the conducted experiments see 118
 Table 1. ¹³C and ¹⁵N resonance assignments were obtained 119
 by using a previously established assignment strategy 120
 based on a sequential walk applying 3D NMR spectra 121
 (Habenstein et al. 2011; Schuetz et al. 2010) which were 122
 analyzed with the software CcpNmr (Fogh et al. 2002; 123
 Stevens et al. 2011; Vranken et al. 2005). Many resonances 124
 were assigned applying conventional experiments, such as 125
 NCACB, NCACX, NCOCX and CANCO. In case of 126
 spectral overlap, it was essential to complement the 127
 assignment strategy with relayed NMR experiments, such 128
 as NcoCACB, CANcoCA and NcaCBCX. Although those 129
 experiments are less sensitive due to four polarization 130
 transfer steps, they strongly benefit from a larger spectral 131
 dispersion (Schuetz et al. 2010), and the signal/noise ratio 132
 achieved under the conditions used here (high field, full 133
 rotor, moderate-sized protein) is good. A selective C’-C α 134
 polarization transfer in those experiments was achieved by 135
 a modified band-selective homonuclear cross-polarization 136
 step (Chevelkov et al. 2013). The spectra used for assign- 137
 ment were all recorded on a single sample, whereas 138
 reproducibility was carefully checked by 2D measurements 139
 on samples from different preparations which yield 140

Table 1 Overview about experimental parameters of the performed solid-state NMR experiments

Experiment	DARR	NCA	NCACB	NCACX	NCOCX
<i>(a)</i>					
MAS frequency/kHz	17.0	17.0	17.5	17.0	17.0
Field/T	20.0	20.0	18.8	20.0	20.0
Transfer I	HC-CP	HN-CP	HN-CP	HN-CP	HN-CP
¹ H field/kHz	59.4	60.8	58.5	60.8	60.8
X field/kHz	40.9	43.1	44.0	43.1	43.1
Shape	Tangent ¹ H	Tangent ¹ H	Tangent ¹ H	Tangent ¹ H	Tangent ¹ H
¹³ C carrier/ppm	95	–	–	–	–
Time/ms	0.5	0.6	0.6	0.6	0.6
Transfer II	DARR	NC-CP	NC-CP	NC-CP	NC-CP
¹ H field/kHz	17.0	–	–	–	–
¹³ C field/kHz	–	6.1	10.0	6.1	6.1
¹⁵ N field/kHz	–	10.2	27.0	10.2	10.6
Shape	–	Tangent ¹³ C	Tangent ¹³ C	Tangent ¹³ C	Tangent ¹³ C
Carrier/ppm	95	60	56	60	178
Time/ms	10	6	4	6	4
Transfer 3	–	–	DREAM	DARR	DARR
¹ H field/kHz	–	–	–	25.1	25.1
¹³ C field/kHz	–	–	7.9	–	–
¹⁵ N field/kHz	–	–	–	–	–
Shape	–	–	Tangent ¹³ C	–	–
Carrier/ppm	–	–	56	178	178
Time/ms	–	–	4	60	30
t1 increments	2000	2000	80	108	108
Sweep width (t1)/kHz	100	66.7	5.7	6.0	6.0
Acquisition time (t1)/ms	10	15	7.1	9.0	9.0
t2 increments	2988	3072	116	136	116
Sweep width (t2)/kHz	100	100	10.9	8.6	6.4
Acquisition time (t2)/ms	14.9	15.4	5.3	8.0	9.0
t3 increments	–	–	1988	3072	3072
Sweep width (t3)/kHz	–	–	100	100	100
Acquisition time (t3)/ms	–	–	9.9	15.4	15.4
¹ H Spinal64 (Fung et al. 2000) decoupling power/kHz	89	89	90	89	89
Inter-scan delay/s	2.1	3	2.5	2.6	2.6
Number of scans	12	8	24	8	8
Measurement time/h	14	13	157	87	74
Experiment	CANCO	NcoCACB	CANcoCA	NcaCBCX	CCC
<i>(b)</i>					
MAS frequency/kHz	17.0	17.0	17.0	17.0	17.5
Field/T	20.0	20.0	20.0	20.0	18.8
Transfer I	HC-CP	HN-CP	HC-CP	HN-CP	HC-CP
¹ H field/kHz	59.4	60.8	58.4	58.4	66.0
X field/kHz	40.9	43.1	40.8	45.2	50.0
Shape	Tangent ¹ H	Tangent ¹ H	Tangent ¹ H	Tangent ¹ H	Tangent ¹ H
¹³ C carrier/ppm	95	–	103	–	58.5
Time/ms	0.5	0.6	0.5	0.6	0.7
Transfer II	CN-CP	NC-CP	CN-CP	NC-CP	DREAM

Table 1 continued

Experiment	CANCO	NcoCACB	CANcoCA	NcaCBCX	CCC
¹ H field/kHz	–	–	–	–	–
¹³ C field/kHz	6.0	6.1	6.0	5.9	5.4
¹⁵ N field/kHz	20.0	10.6	11.4	11.4	–
Shape	Tangent ¹³ C	Tangent ¹³ C	Tangent ¹³ C	Tangent ¹³ C	Tangent ¹³ C
¹³ C Carrier/ppm	60	178	60	60	56
Time/ms	4	4	5.5	5.5	4
Transfer 3	NC-CP	Mod. band-selective CP (Chevelkov et al. 2013)	NC-CP	DREAM	DARR
¹ H field/kHz	–	–	–	–	17.5
¹³ C field/kHz	6.0	8.5	6.0	7.6	–
¹⁵ N field/kHz	20.0	–	11.9	–	–
Shape	Tangent ¹³ C	Tangent ¹³ C	Tangent ¹³ C	Tangent ¹³ C	–
¹³ C Carrier/ppm	178	176	178	51	40
Time/ms	4	–	3.5	2	80
Transfer 4	–	DREAM	Mod. band-selective CP (Chevelkov et al. 2013)	DREAM	–
¹ H field/kHz	–	–	–	–	–
¹³ C field/kHz	–	7.7	8.3	7.6	–
¹⁵ N field/kHz	–	–	–	–	–
Shape	–	Tangent ¹³ C	Tangent ¹³ C	Tangent ¹³ C	–
¹³ C Carrier/ppm	–	51	178	26	–
Time/ms	–	2.75	5	4	–
t1 increments	130	62	150	68	172
Sweep width (t1)/kHz	8.5	3.4	8.6	4.3	15.7
Acquisition time (t1)/ms	7.6	9.0	8.8	7.9	5.5
t2 increments	98	154	80	156	172
Sweep width (t2)/kHz	6.03	8.6	4.3	12.8	15.7
Acquisition time (t2)/ms	8.1	9.0	9.3	6.1	5.5
t3 increments	3072	3072	3072	3072	1864
Sweep width (t3)/kHz	100	100	100	100	93.8
Acquisition time (t3)/ms	15.3	15.4	15.4	15.4	9.9
¹ H Spinal64 (Fung et al. 2000) decoupling power/kHz	89.0	89.0	91.1	91.1	90.0
Inter-scan delay/s	2.7	3	3	3	2.1
Number of scans	8	16	16	16	8
Measurement time/h	77	128	162	143	145

141 comparable spectra in all cases. Spectra were also recorded
142 on samples with the His-tag, and showed differences large
143 enough to discard the further use of this sample.

144 TALOS+ calculations were performed using version 3.8
145 (Shen et al. 2009). The DSSP algorithm (Kabsch and
146 Sander 1983) was applied using the corresponding web
147 interface (<http://www.cmbi.ru.nl/dssp.html>) with the 3D
148 atomic coordinates extracted from the pdb file 3GXV
149 (Kashav et al. 2009).

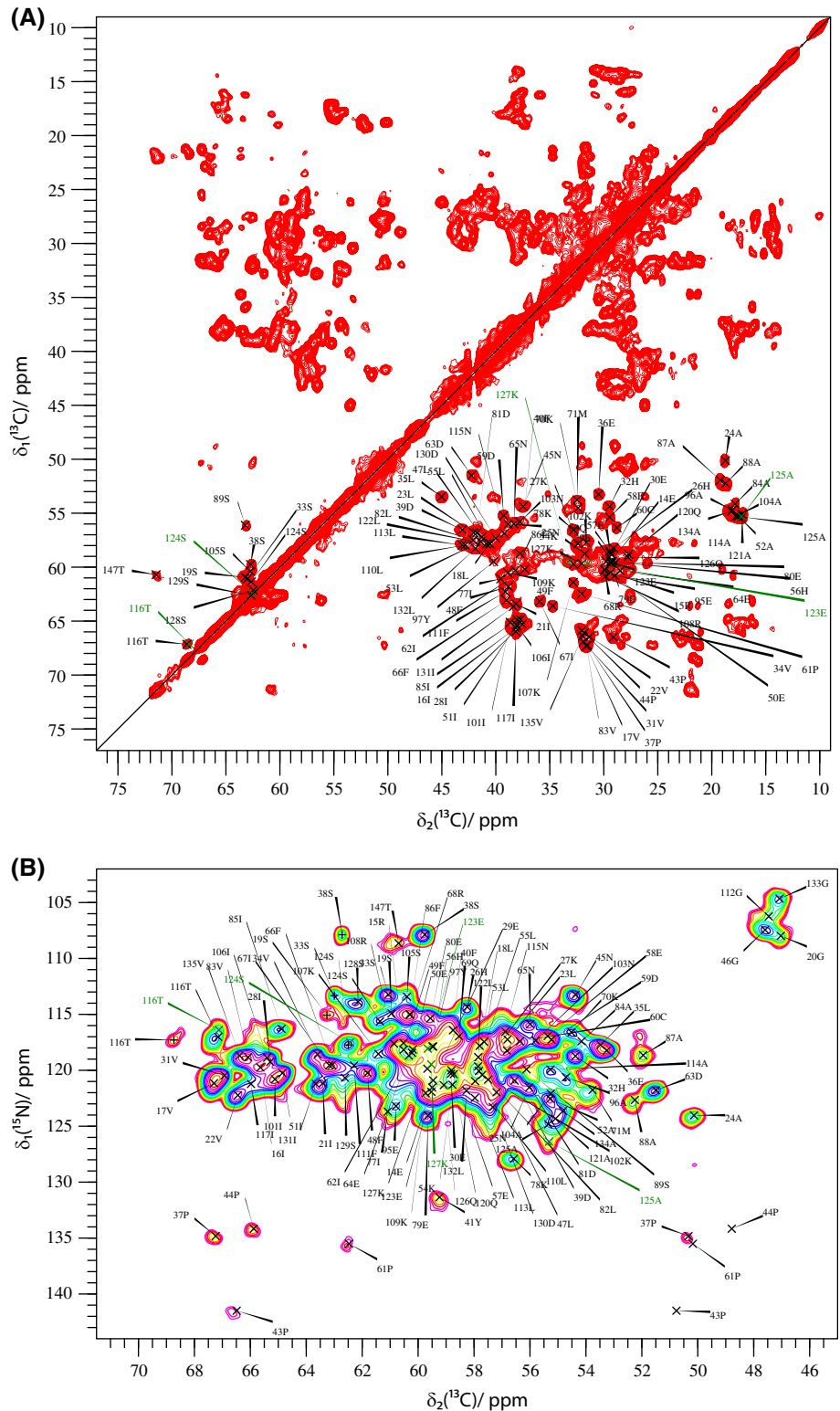
150 Solid-state FLYA calculations (Schmidt et al. 2013;
151 Schmidt and Güntert 2012) were performed with CYANA
152 version 3.97. The tolerance value for chemical shift

153 matching was set to 0.55 ppm for ¹³C and ¹⁵N. The cal-
154 culations are based on experimental peak lists as obtained
155 from the manual assignment procedure.

Assignment and data deposition 156

157 The solid-state NMR spectra of the N-terminal domain of
158 *HpDnaB* (residues 1–153) reveal significant spectral
159 overlap as expected for a protein of 153 amino acids, even
160 though also many isolated, well resolved signals are
161 detected as can be seen in the 2D dipolar correlation NMR

Fig. 2 **a** 2D $^{13}\text{C},^{13}\text{C}$ DARR spectrum of the N-terminus of *HpDnaB* measured at 20.0 T with a spinning frequency of 17.0 kHz and 10 ms DARR mixing. The spectrum includes the labels for the $\text{C}\alpha$ - $\text{C}\beta$ peaks as predicted from the manually created shift list using the CcpNmr software (*black chain A, green chain B*). In the $\text{C}\alpha/\text{C}\beta$ region seven isolated peaks could not be assigned, most probably because the corresponding residues are located in flexible parts of the protein. **b** 2D NCA spectrum of the N-terminus of *HpDnaB* acquired at 20.0 T with a spinning frequency of 17.0 kHz. The spectrum includes the labels for the peaks as predicted from the manually created shift list using the CcpNmr software (*black chain A, green chain B*) assuming that only intraresidual peaks with a through-space limit corresponding to one bond are visible (x), peaks labeled with *plus* indicate N-C β resonances



162 spectra shown in Fig. 2. Those ^{13}C resonances are quite
 163 narrow with a line width at half height in the order of
 164 0.6 ppm. Figure 2a shows the 2D $^{13}\text{C},^{13}\text{C}$ DARR spectrum and Fig. 2b the 2D $^{15}\text{N},^{13}\text{C}$ NCA spectrum, both with good

166 signal-to-noise ratio which allows also to acquire 3D
 167 assignment NMR spectra even with four polarization-
 168 transfer steps. The assignment was mainly achieved by
 169 using a combination of two strategies. The first one is based

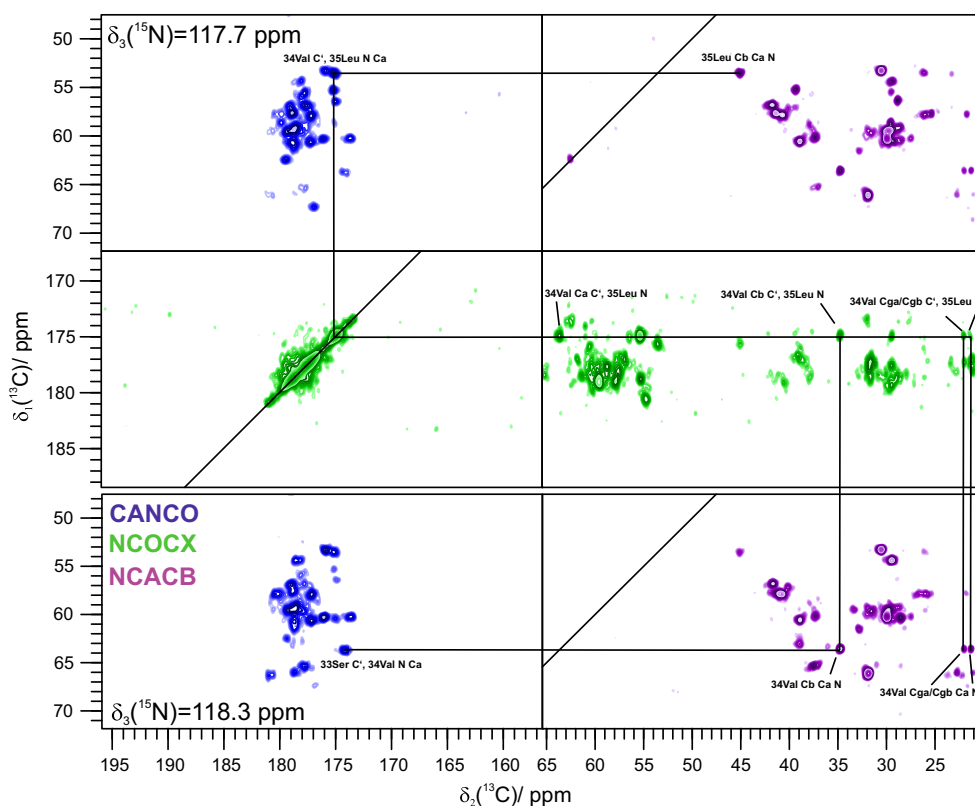


Fig. 3 Example for the sequential walk along the protein backbone (from the C- to the N-terminus) by using NCACB (negative peaks are shown in *magenta*), CANCO (positive peaks are illustrated in *blue*) and NCOCX (positive peaks are shown in *green*) spectra

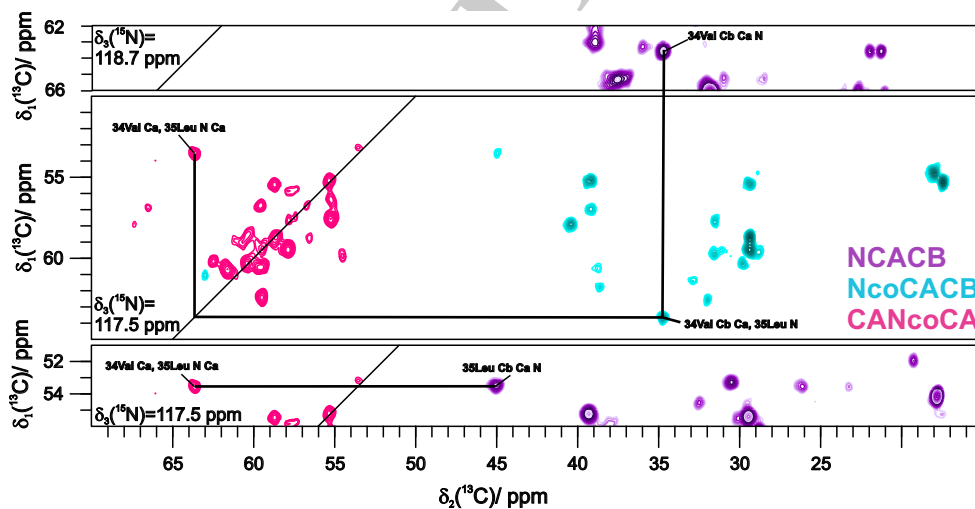


Fig. 4 Example for the sequential walk along the protein backbone (from the N- to the C-terminus) of the N-terminus of DnaB by using NCACB (negative peaks represented in *magenta*), NcoCACB

(negative peaks shown in *turquoise*) and CANcoCA (positive peaks represented in *pink*) spectra

170 on 3D NMR spectra such as NCACB, NCACX, NCOCX
171 and CANCO (Schuetz et al. 2010). A representative
172 example for the backbone walk using this “classical”
173 strategy is given in Fig. 3. The spectral overlap observed in
174 the NMR spectra requires the largest possible spectral

dispersion in all dimensions, which is in terms of 3D NMR
spectra given by circumventing the detection of the CO-
dimension which possesses the smallest chemical shift
dispersion. For fulfilling this objective, an assignment
strategy based on NCACB, NcoCACB and CANcoCA

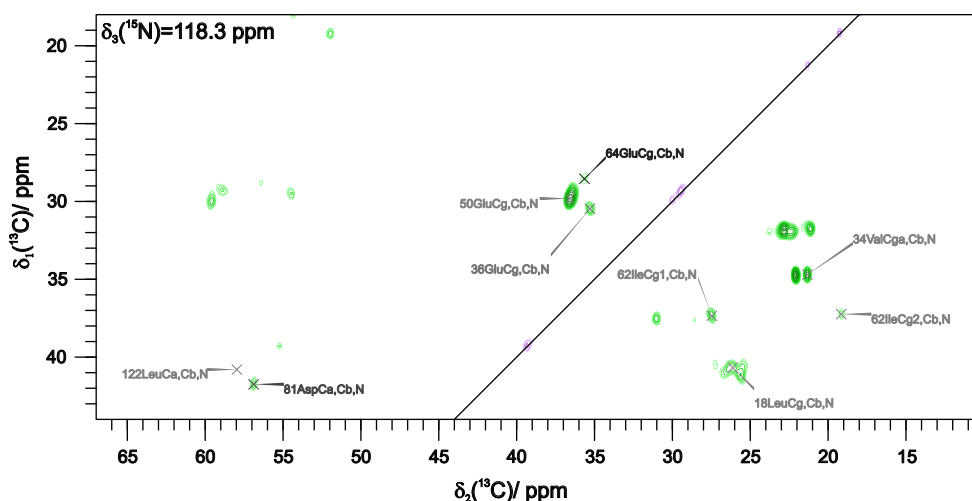


Fig. 5 Example of a representative plane extracted from the 3D NcaCBCX spectrum ($\delta(^{15}\text{N}) = 118.3$ ppm) used for side-chain assignment

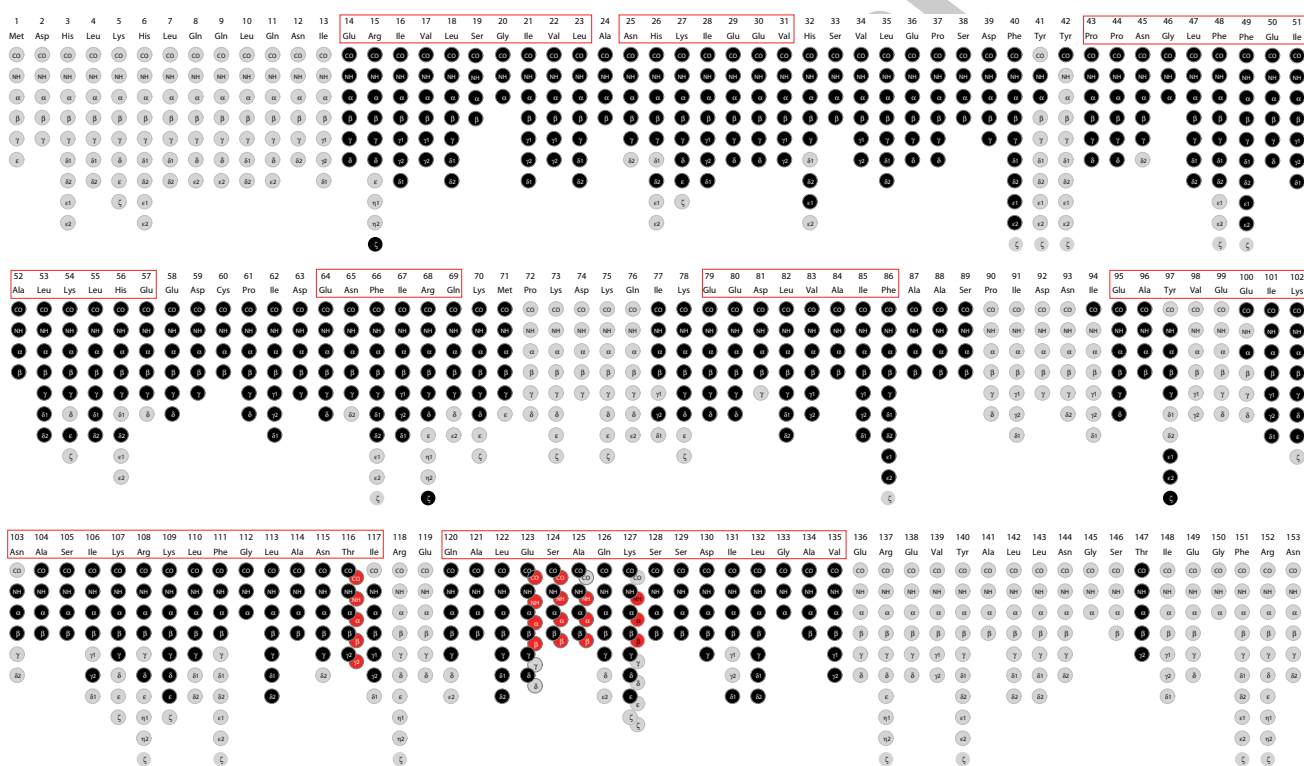


Fig. 6 Assignment graph of the N-terminus of *HpDnaB* created using the CcpNmr software. Residues marked in red show significant peak doubling. Black or red dots indicate assigned spins, grey dots

unassigned spins. Residues highlighted by red rectangles are located in α -helices as determined from NMR secondary chemical shifts (see Fig. 9)

180 experiments (Schuetz et al. 2010) was applied, a repre-
 181 sentative example of a sequential walk is given in Fig. 4.
 182 This assignment procedure could clarify many assignments
 183 which remained ambiguous after the firstly described
 184 assignment strategy. The selective $C' \rightarrow C\alpha$ polarization
 185 transfer step in the relayed experiments (Chevelkov et al.
 186 2013) yields a good signal-to-noise ratio also for these

187 types of experiments (see Fig. 4). Nevertheless, it has to be
 188 noted that a small number of resonances could not be
 189 assigned, mainly due to the spectral overlap as especially
 190 visible in the leucine, glutamic acid and glutamine region.
 191 The sidechains are mainly assigned by analyzing CCC
 192 (DREAM and DARR transfer) and NcaCBCX (two
 193 DREAM transfers) spectra (see Fig. 5). On basis of the

Table 2 Statistics of the manually performed peak assignments

Category	Assigned/%
C	69.3
CA	70.6
CB	69.4
CG	61.7
CD	54.5
CE	34.5
CZ	17.6
N	69.9
Residue Ala	91.7
Residue Arg	50.0
Residue Asn	55.6
Residue Asp	62.5
Residue Cys	100.0
Residue Gln	42.9
Residue Glu	72.2
Residue Gly	66.7
Residue His	60.0
Residue Ile	81.3
Residue Leu	68.8
Residue Lys	72.7
Residue Met	50.0
Residue Phe	85.7
Residue Pro	66.7
Residue Ser	88.9
Residue Thr	100.0
Residue Tyr	75.0
Residue Val	75.0

Data created with the CcpNmr software

194 acquired spectra and the applied assignment strategies,
 195 approximately 70 % of the backbone carbon and nitrogen
 196 atoms could be assigned (see Fig. 6; Table 2). 77 % of the
 197 residues for which ^{15}N , $^{13}\text{C}\alpha$ and $^{13}\text{C}\beta$ chemical shifts were
 198 assigned are located in α -helices as indicated by the NMR
 199 results (vide infra). The resonances of most of the unassigned
 200 residues could not be detected in the 3D NMR
 201 spectra, most probably because they are located in flexible
 202 parts of the protein (those resonances were also not
 203 detected in $^{13}\text{C}, ^1\text{H}$ INEPT and $^{15}\text{N}, ^1\text{H}$ HSQC spectra
 204 indicating intermediate dynamics in this protein). Notably,
 205 the resonances of Thr147 are clearly detected in the 2D
 206 DARR spectrum (see Fig. 2a), but appear only very weakly
 207 in the 3D NCACB and CCC spectra and are even absent in
 208 the other 3D NMR spectra. Since the second threonine
 209 residue (Thr116) present in the N-terminus of *HpDnaB*
 210 could be assigned on the basis of the before described
 211 assignment strategies, the remaining Thr signal can be
 212 assigned to Thr147, and weak correlations visible in the 2D
 213 DARR spectrum at long mixing times support this

conclusion. The $\text{C}\alpha$ and $\text{C}\beta$ chemical shifts of these two
 214 threonine residues already reveal that Thr116 is located in
 215 an α -helix, whereas Thr147 is most probably located in a
 216 loop in agreement with the observed flexible character. The
 217 chemical shifts have been deposited in the BMRB database
 218 under the accession number 26548. 219

As indicated in Fig. 6, for some resonances in the
 220 amino-acid region Thr116-Lys127 a peak doubling is
 221 observed which is exemplarily illustrated by analyzing the
 222 unique serine-alanine amino acid pair (residues Ser124 and
 223 Ala125). The sequential backbone walk for these residues
 224 using NCACB, NcoCACB and CANcoCA spectra is
 225 illustrated in Fig. 7 and clearly demonstrates the presence
 226 of two sets of resonances. Pronounced spectroscopic dif-
 227 ferences are mainly observed for the ^{15}N frequencies. The
 228 observed peak doubling might indicate crystallographically
 229 distinct molecules in the asymmetric unit, which would
 230 agree with the previously published crystal structure for the
 231 residues 1–121 consisting of a dimer in the asymmetric unit
 232 (Kashav et al. 2009). 233

The results of the manual assignment procedure are
 234 validated by automated peak assignments as implemented
 235 in the solid-state FLYA algorithm (Schmidt et al. 2013).
 236 Figure 8 illustrates the good agreement between the man-
 237 ually assigned residues and the assignments obtained by
 238 FLYA calculations based on the peak lists from the manual
 239 assignment procedure. Only a few significant differences
 240 (e.g. for the two prolines Pro43 and Pro44, as well as for
 241 Thr147, and the C' resonances of Ser89 and Val135) were
 242 observed and in those cases the manually assignment was
 243 carefully rechecked and its resonances were taken for the
 244 final assignment as they unambiguously result from the
 245 performed sequential walk. 246

247 Secondary structure

248 Secondary chemical shifts were obtained by subtracting the
 249 random-coil shifts (Wang and Jardetzky 2002) from the
 250 observed solid-state NMR chemical shifts (Wishart et al.
 251 1992) and are visualized in Fig. 9. These data clearly
 252 illustrate the dominant α -helical character of the N-terminus
 253 of *HpDnaB*. Seven α -helices are identified in total, the
 254 longest one is reaching from residue 95 to 117. Our results
 255 indicate an interruption after the sixth α -helix and a suc-
 256 ceeding seventh α -helix with positive secondary chemical
 257 shifts observed for residues 120–135. It is reasonable to
 258 assume that the C-terminal part of the protein is mainly
 259 flexible, since most resonances are not detected in the
 260 performed NMR experiments. The visible residue Thr147
 261 shows $\text{C}\alpha/\text{C}\beta$ chemical shifts more typical for a loop or
 262 extended conformation than an α -helical arrangement
 263 (Wang and Jardetzky 2002). The secondary chemical shifts

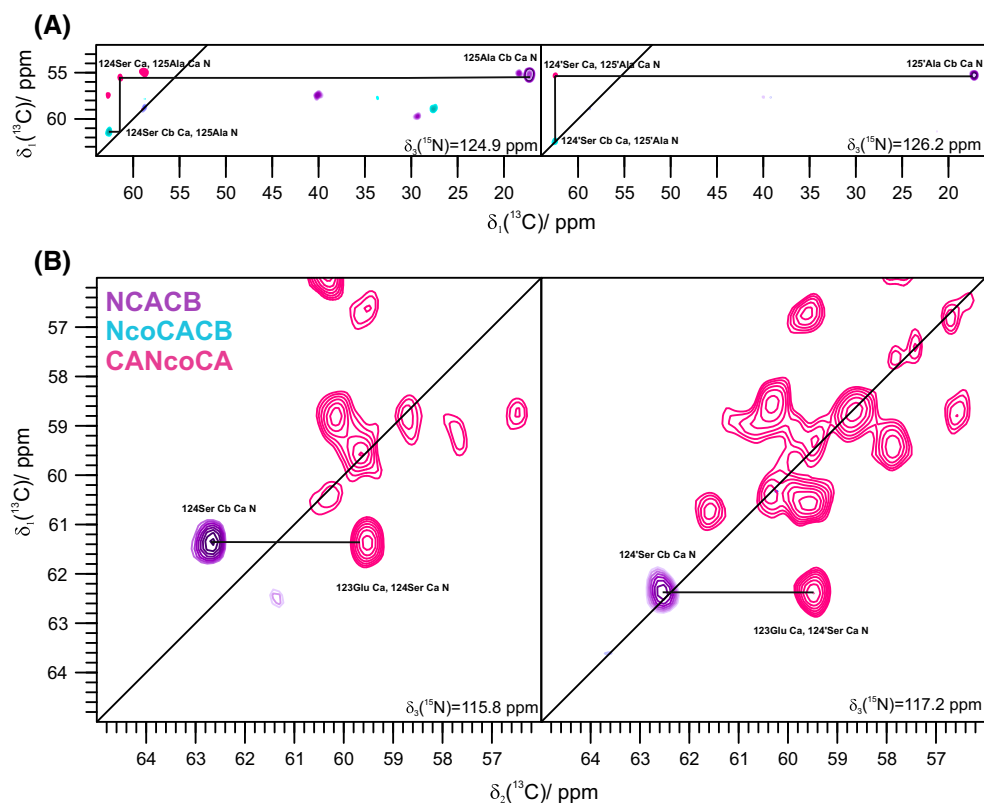


Fig. 7 Illustration of peak doubling for a unique Ser-Ala amino acid pair (124Ser-125Ala). **a** The sequential walk along the protein backbone based on NcoCACB (negative peaks are illustrated in turquoise), CANcoCA (positive peaks are shown in pink) and

NCACB (negative peaks are shown in magenta) spectra is shown for the two sets of resonances. **b** Correlation between the residues Ser124 and Glu123 in the NCACB and CANcoCA spectra, for the color code see (a)

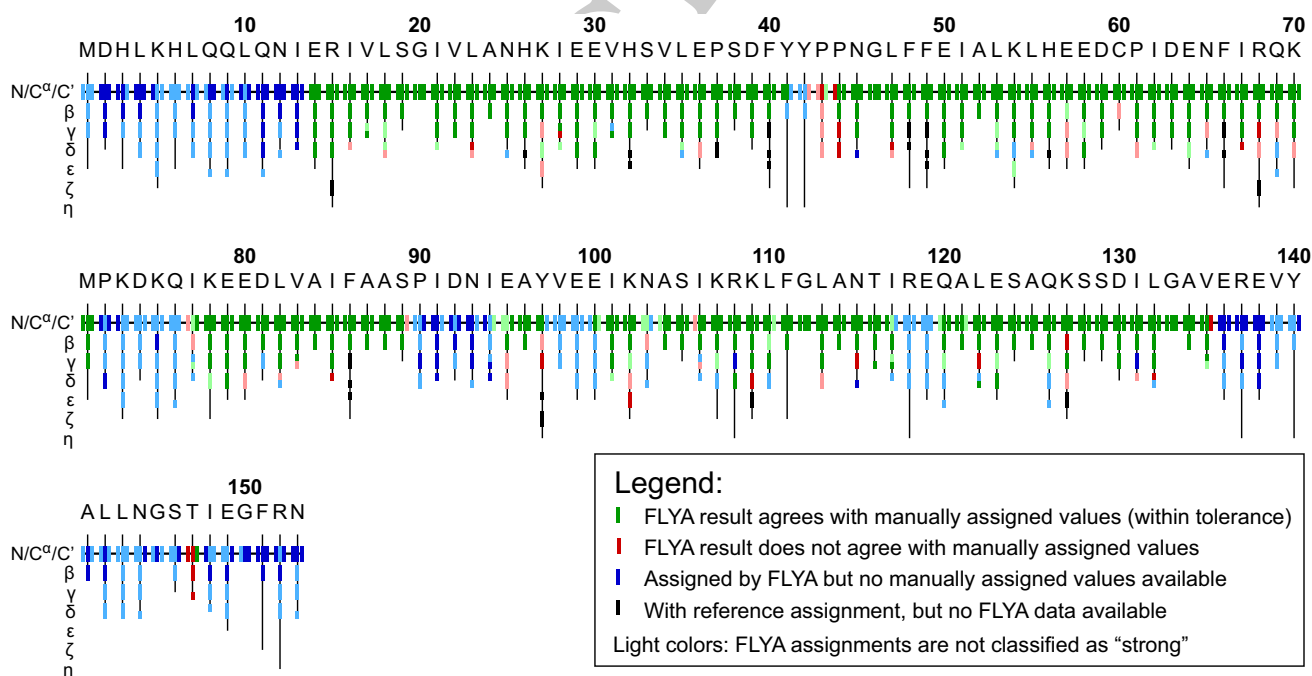


Fig. 8 Result of an automated peak assignment using ssFLYA calculations on the basis of the manually created peak lists (which were used for the sequential assignment) extracted from NCACB, CANCO, NCOCX, NCACO, CANcoCA, NcoCACB and NcaCBCX spectra

Fig. 9 Secondary ^{13}C chemical shifts (obtained by subtracting the random-coil shifts (Wang and Jardetzky 2002) from the observed chemical shifts). Glycines are marked in *black* (and $\Delta\delta\text{C}\alpha$ is plotted) and residues for which significant peak doubling was observed are highlighted with a+

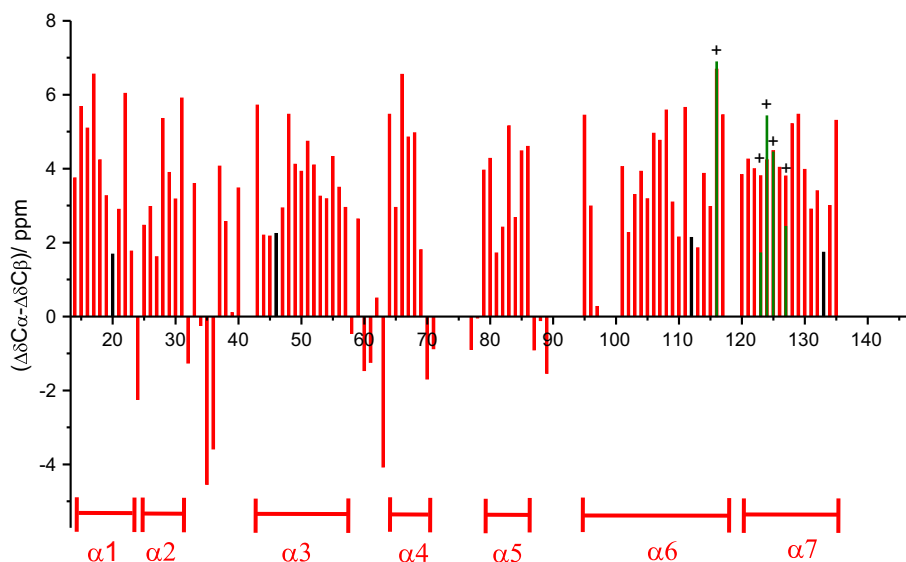


Table 3 α -Helices determined from the secondary chemical shifts and from the 3D atomic coordinates deposited in the pdb file 3GXV using the DSSP algorithm (Kabsch and Sander 1983) via the corresponding web interface

α -Helix	NMR	TALOS+ ^a	DSSP ^b
1	Glu14-Leu23	Arg15-Leu23	His3-Leu23
2	Asn25-Val31 ^c	His26-His32	Ile28-His32 ^d
3	Pro43-Glu57	Pro44-Glu57	Pro43-Glu57
4	Glu64-Gln69	Glu64-Gln69	Glu64-Gln69
5	Glu79-Phe86	Glu79-Phe86	Glu79-Phe86
6	Glu95-Ile117	Ile101-Ile117	Glu95-Gln120
7	120Gln-135Val	120Gln-135Val	-

^a Calculated from the solid-state NMR chemical shifts described in this work using the TALOS+ software (Shen et al. 2009)

^b Data for chain A are given

^c Data do not allow a distinction between 3/10 helix and α -helix

^d A 3/10 helix is predicted for residues Asn25-Lys27

264 for the doubled resonances have the same sign and
265 approximate magnitude for both partners, indicating no
266 significant differences in the secondary structure elements
267 (see Fig. 9).

268 A complete comparison of the secondary structure ele-
269 ments obtained from solid-state NMR with those found in
270 the published crystal structure is hampered by the fact that
271 the latter one consists only of residues 1–121 (Kashav et al.
272 2009) and might crystallize differently than the full-length
273 N-terminal domain (no diffracting crystals could be
274 obtained for the full-length N-terminal domain). Never-
275 theless, the structure of the globular N-terminal domain
276 seems to be roughly similar between the 1–121 and 1–153
277 residues samples, since in general a good agreement
278 between NMR data [secondary chemical shifts and

TALOS+ backbone torsion angle calculations (Shen et al. 279
2009)] and the X-Ray structure is observed (see Table 3). 280

Conclusions 281

282 We describe the sequential resonance assignment of the
283 N-terminal domain of *HpDnaB* (residues 1–153) based on
284 3D solid-state NMR experiments leading to a site-specific
285 chemical shift assignment of approximately 70 % of the
286 backbone resonances. Those manually obtained peak
287 assignments are validated by solid-state FLYA calcula-
288 tions. Seven α -helices were identified by a secondary
289 chemical shift analysis which mostly agrees with the single
290 crystal structure published for the residues 1–121 (PDB
291 3GXV). The observed peak doubling might point to crys-
292 tallographically distinct molecules in the asymmetric unit.

293 **Acknowledgments** This work was supported by the Agence
294 Nationale de la Recherche (ANR-11-BSV8-021-01, ANR-12-BS08-
295 0013-01), the ETH Zurich, the Swiss National Science Foundation
296 (Grant 200020_159707 and 200020_146757). PG is supported by the
297 Lichtenberg Program of the Volkswagen Foundation, AB and LT by
298 the CIBLE program 2011 from the Région Rhône-Alpes.

References 299

- 300 Stelter M et al (2012) Structure 20:554
301 Böckmann A et al (2009) Characterization of different water pools in
302 solid-state NMR protein samples. J Biomol NMR 45:319–327
303 Chevelkov V, Giller K, Becker S, Lange A (2013) Efficient CO–CA
304 transfer in highly deuterated proteins by band-selective homonu-
305 clear cross-polarization. J Magn Reson 230:205–211
306 Corn JE, Berger JM (2006) Regulation of bacterial priming and
307 daughter strand synthesis through helicase–primase interactions.
308 Nucleic Acids Res 34:4082–4088

- 309 Fogh R et al (2002) The CCPN project: an interim report on a data
310 model for the NMR community. *Nat Struct Mol Biol* 9:416–418
311 Fung BM, Khitirin AK, Ermolaev K (2000) An improved broadband
312 decoupling sequence for liquid crystals and solids. *J Magn Reson*
313 142:97–101
- 314 Gardiennet C, Schütz AK, Hunkeler A, Kunert B, Terradot L,
315 Böckmann A, Meier BH (2012) A sedimented sample of a
316 59 kDa dodecameric helicase yields high-resolution solid-state
317 NMR spectra. *Angew Chem Int Ed* 51:7855–7858
- 318 Gor'kov PL, Witter R, Chekmenev EY, Nozirov F, Fu R, Brey WW
319 (2007) Low-E probe for 19F–1H NMR of dilute biological
320 solids. *J Magn Reson* 189:182–189
- 321 Habenstein B et al (2011) Extensive de novo solid-state NMR
322 assignments of the 33 kDa C-terminal domain of the Ure2 prion.
323 *J Biomol NMR* 51:235–243
- 324 Kabsch W, Sander C (1983) Dictionary of protein secondary
325 structure: pattern recognition of hydrogen-bonded and geomet-
326 rical features. *Biopolymers* 22:2577–2637
- 327 Kashav T, Nitharwal R, Abdulrehman SA, Gabdoulkhakov A,
328 Saenger W, Dhar SK, Gourinath S (2009) Three-dimensional
329 structure of N-terminal domain of DnaB helicase and helicase–
330 primase interactions in *Helicobacter pylori*. *PLoS One* 4:e7515
- 331 LeBowitz JH, McMacken R (1986) The *Escherichia coli* dnaB
332 replication protein is a DNA helicase. *J Biol Chem* 261:
333 4738–4748
- 334 Nitharwal RG et al (2007) The domain structure of *Helicobacter*
335 *pylori* DnaB helicase: the N-terminal domain can be dispensable
336 for helicase activity whereas the extreme C-terminal region is
337 essential for its function. *Nucleic Acids Res* 35:2861–2874
- 338 Parsonnet J, Friedman GD, Vandersteen DP, Chang Y, Vogelman JH,
339 Orentreich N, Sibley RK (1991) *Helicobacter pylori* infection
340 and the risk of gastric carcinoma. *N Engl J Med* 325:1127–1131
- 341 Peterson WL (1991) *Helicobacter pylori* and peptic ulcer disease.
342 *N Engl J Med* 324:1043–1048
- Schmidt E, Güntert P (2012) A new algorithm for reliable and general
NMR resonance assignment. *J Am Chem Soc* 134:12817–12829
- Schmidt E et al (2013) Automated solid-state NMR resonance
assignment of protein microcrystals and amyloids. *J Biomol*
NMR 56:243–254
- Schuetz A et al (2010) Protocols for the sequential solid-state NMR
spectroscopic assignment of a uniformly labeled 25 kDa protein:
HET-s(1–227). *ChemBioChem* 11:1543–1551
- Shen Y, Delaglio F, Cornilescu G, Bax A (2009) TALOS+: a hybrid
method for predicting protein backbone torsion angles from
NMR chemical shifts. *J Biomol NMR* 44:213–223
- Soni RK, Mehra P, Choudhury NR, Mukhopadhyay G, Dhar SK
(2003) Functional characterization of *Helicobacter pylori* DnaB
helicase. *Nucleic Acids Res* 31:6828–6840
- Soni RK, Mehra P, Mukhopadhyay G, Dhar SK (2005) *Helicobacter*
pylori DnaB helicase can bypass *Escherichia coli* DnaC function
in vivo. *Biochem J* 389:541–548
- Stevens T et al (2011) A software framework for analysing solid-state
MAS NMR data. *J Biomol NMR* 51:437–447
- Studier FW (2005) Protein production by auto-induction in high-
density shaking cultures. *Protein Expr Purif* 41:207–234
- The UniProt Consortium—Activities at the Universal Protein Resource
(UniProt) (2014) *Nucleic Acids Res* 42:D191–D198
- Vranken WF et al (2005) The CCPN data model for NMR
spectroscopy: development of a software pipeline. *Proteins*
Struct Funct Bioinform 59:687–696
- Wang Y, Jardetzky O (2002) Probability-based protein secondary
structure identification using combined NMR chemical-shift
data. *Protein Sci* 11:852–861
- Wishart DS, Sykes BD, Richards FM (1992) The chemical shift
index: a fast and simple method for the assignment of protein
secondary structure through NMR spectroscopy. *Biochemistry*
31:1647–1651

UNCORRECTED

Journal : **12104**

Article : **9629**

Author Query Form

Please ensure you fill out your response to the queries raised below and return this form along with your corrections

Dear Author

During the process of typesetting your article, the following queries have arisen. Please check your typeset proof carefully against the queries listed below and mark the necessary changes either directly on the proof/online grid or in the 'Author's response' area provided below

Query	Details Required	Author's Response
AQ1	Please check and confirm that the authors and their respective affiliations have been correctly identified and amend if necessary.	
AQ2	Please provide article title for the references Stelter et al. (2012) and The UniProt Consortium-Activities at the Universal Protein Resource (UniProt) (2014).	